

UNFALSIFIED CONTROL USING AN ELLIPSOIDAL UNFALSIFIED REGION APPLIED TO A MOTION SYSTEM

Jeroen van Helvoort,* Bram de Jager,*
Maarten Steinbuch *

* *Technische Universiteit Eindhoven, Department of Mechanical
Engineering, P.O. Box 513, 5600 MB Eindhoven, The
Netherlands, E-mail: j.j.m.v.helvoort@tue.nl*

Abstract: In this paper, unfalsified control theory (a data-driven model-free control theory) is applied to determine which control parameter sets in a specified control structure are able to meet a given performance specification, using merely measured input/output data. The need for a finite, often large, amount of parameter sets (“gridding”) is overcome by applying an ellipsoidal description of the region containing all unfalsified control parameter sets (the “unfalsified region”). It is shown that by using an appropriate performance specification, the optimal update of the ellipsoidal unfalsified region, initiated by new data, can be computed analytically.

With the two properties mentioned, improved convergence and reduction of computational effort are combined to derive the unfalsified control parameter set. Real-time implementation is demonstrated by experimental results obtained on a motion system.
Copyright ©2005 IFAC

Keywords: Unfalsified control, Model-free, Self-adaptive control, Self-tuning control

1. INTRODUCTION

The concept of unfalsified control was introduced by Safonov and Tsao (1994) as “a framework for determining control laws whose ability to meet given performance specification is at least not invalidated (i.e., not falsified) by the experimental data.” This data-driven model-free control approach recursively falsifies control parameter sets that fail to satisfy a performance specification, given measured data and specified control law. The only assumption is that at least one controller from the original controller pool satisfies the performance specification at all times.

Although in early works the parameter space was gridded (resulting in a finite set of candidate controllers), this restriction was lifted by Cabral and Safonov (2003) by applying a quadratic performance specification to a control law where the control parameters appear affine. Hence, the region of unfalsi-

fied control parameter sets is specified by an ellipsoid $\mathcal{E}(t_{k-1})$. New measurements define a new ellipsoid $\mathcal{F}(t_k)$, and the intersection of both ellipsoids specifies the region containing the unfalsified control parameter sets including the information of the new measurement. This intersection is approximated by an outer-bounding ellipsoid $\mathcal{E}(t_k)$, to ensure that no unfalsified parameter set is wrongly falsified and that an ellipsoidal unfalsified region is maintained. In (Cabral and Safonov, 2003), this outer-bounding ellipsoid is calculated by the ellipsoid algorithm (Boyd *et al.*, 1994).

The major drawback of the ellipsoid algorithm, as applied by Cabral and Safonov (2003), is that the algorithm uses a cutting plane through the center of the ellipsoid and hence this cutting plane can only be applied when the current control parameter set (center of the ellipsoid $\mathcal{E}(t_{k-1})$) is falsified. When it is unfalsified, the ellipsoid is not changed and the newly ac-

quired unfalsification information is discarded, which results in a slow convergence. Other algorithms can be used, to tighter bound the approximation of the intersection of the two ellipsoids to improve convergence, however, as stated by Henrion *et al.* (1998), “the problem of describing the ellipsoid of smallest volume that contains the intersection of given ellipsoids is NP-hard.” Solutions often rely on iterative optimization procedures (such as LMI optimizations) and, although subject to extensive research for many years, only in a few exceptional cases the exact solution is known. The exact solutions are known, for instance, when the ellipsoid is exactly sliced in half (as is employed by Cabral and Safonov (2003)), when the centers of two intersecting ellipsoids coincide, or when at least one ellipsoid degenerates into two parallel half-spaces (Pronzato and Walter, 1994; Ros *et al.*, 2002; Maksarov and Norton, 1996; Katsaggelos *et al.*, 2001). When these methods are applied to intersections which do not fulfill these conditions, an outer-bounding ellipsoid will result, however, it will not be of minimal volume, resulting in slow convergence. Summarizing, either the convergence is slow, or the intersection procedure is computationally demanding.

This paper shows that, by choosing an appropriate ℓ_∞ performance specification, the ellipsoid $\mathcal{F}(t_k)$ defined by new measurement data degenerates into two half-spaces, whose intersection with a general ellipsoid can be optimally approximated by a minimum-volume outer-bounding ellipsoid. This ellipsoid can be computed analytically (e.g., by the Ellipsoid-with-Parallel-Cuts algorithm as proposed by Pronzato and Walter (1994)). Consequently,

- the convergence is faster because the current control parameter set doesn’t need to be falsified to update the unfalsified region, and moreover, two cutting planes are defined, neither of which is restricted to pass through the center of the ellipsoid.
- the computation of the updated unfalsified region is fast and can be implemented in real time, as is shown in an experiment on a motion system.

To the authors knowledge, no experimental results applying unfalsified control were presented before.

In Section 2 the model reference unfalsified control theory is stated and it is shown that with an appropriate ℓ_∞ performance specification, the ellipsoid $\mathcal{F}(t_k)$ degenerates into two parallel half-spaces. Several control parameter update scenarios are given. In Section 3 the Ellipsoid-with-Parallel-Cuts algorithm, which is used to analytically compute the update of the unfalsified region, is discussed. Section 4 provides a simulation example while Section 5 presents experiments with unfalsified control applied to a motion system. Finally, Section 6 contains conclusions.

2. MODEL REFERENCE UNFALSIFIED CONTROL

2.1 General Setup

In Fig. 1 a blockscheme of a general model reference unfalsified control problem is shown. The plant P is unknown, but its input $u(t)$ and $y(t)$ can be measured.

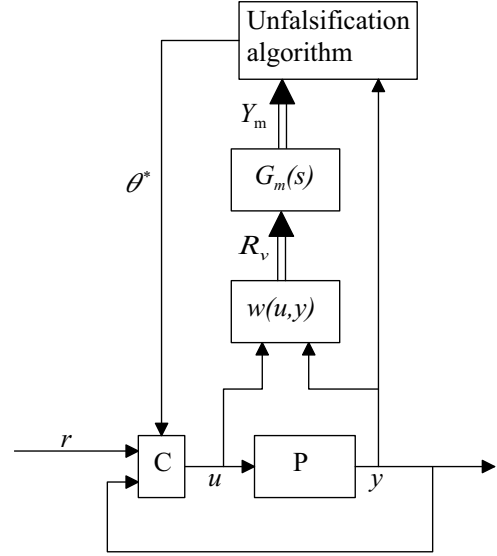


Fig. 1. Blockscheme of a general model reference unfalsified control problem.

Controller C has the structure

$$r(t) = w(u(t), y(t))^T \theta^*(t) \quad (1)$$

with $\theta^*(t)$ the set of p current control parameters and $w(u(t), y(t))$ a p -dimensional vector field with arguments depending on current and past values of $u(t)$ and $y(t)$. Vector field $w(u(t), y(t))$ should be constructed such that $u(t)$ can be determined uniquely from (1), given $r(t)$, $y(t)$, $\theta^*(t)$ and past values of $u(t)$ and $y(t)$.

Define the set of virtual references $R_v(t)$ as

$$R_v(t) = \{r_v(t) = w(u(t), y(t))^T \theta | \theta \in \mathbb{R}^p\} \quad (2)$$

Hence, for every $\theta \in \mathbb{R}^p$, the virtual reference $r_v(t) \in R_v(t)$ results exactly in the measured $u(t)$ and $y(t)$, if that control parameter set θ were in the feedback loop at the time of the measurement.

Let $G_m(s)$ define a stable reference model for the desired closed loop behavior. The set of reference outputs $Y_m(t)$ is defined as

$$\begin{aligned} Y_m(t) &= \{y_m(t) = G_m(s)r_v(t) | r_v(t) \in R_v(t)\} \\ &= \{y_m(t) = G_m(s)w(u(t), y(t))^T \theta | \theta \in \mathbb{R}^p\} \end{aligned} \quad (3)$$

Note that this is a more general setting than without a reference model, since if no reference model is wanted, $G_m(s)$ can be set to 1.

2.2 Performance Specification

Definition (Safonov and Tsao, 1997) A controller is said to be *falsified* by measurement information if this information is sufficient to deduce that the performance specification would be violated, if that controller were in the feedback loop. Otherwise the controller is said to be *unfalsified*.

Consider the ℓ_∞ performance specification given by

$$|L(s)(y(t) - y_m(t))| \leq \Delta(t) \quad \forall t \quad (4)$$

with $L(s)$ some stable filter (e.g., some low-pass filter to reject noise) and $\Delta(t) > 0$ a time and/or reference dependent threshold value. Then the region of control parameter sets that is unfalsified by the current data, $\mathcal{F}(t)$, is given by

$$\mathcal{F}(t) = \{\theta \mid -\Delta(t) \leq L(s) \cdot (y(t) - G_m(s)w(u(t), y(t))^T \theta) \leq \Delta(t)\} \quad (5)$$

which clearly defines two half-spaces. This can also be written as the degenerate ellipsoid

$$\mathcal{F}(t) = \left\{ \theta \mid \left(L(s)(y(t) - G_m(s)w(u(t), y(t))^T \theta) \right)^2 \leq \Delta^2(t) \right\} \quad (6)$$

2.3 Intersection

The region of unfalsified control parameter sets at time $t = t_k$, $\mathcal{E}(t_k)$, is defined by the intersection of the region of unfalsified control parameter sets at time $t = t_{k-1}$, $\mathcal{E}(t_{k-1})$, and the region of control parameter sets that are unfalsified by the new measurement data $\mathcal{F}(t_k)$:

$$\mathcal{E}(t_k) = \mathcal{E}(t_{k-1}) \cap \mathcal{F}(t_k) \quad (7)$$

This intersection will be approximated by an outer-bounding minimal-volume ellipsoid, as is described in section 3.

2.4 Control Parameters Update

The current control parameter set θ^* is falsified at time $t = t_k$ if it is not within the ellipsoid $\mathcal{E}(t_k)$. In that case it needs to be updated, for which several scenarios are possible:

- (1) The center of the ellipsoidal unfalsified region can be taken as new control parameter set. By applying this update law, the new control parameter set will be as far away from the unfalsified bounds as possible. However, the switching might be ‘aggressive’ since the parameter sets could be far apart.

- (2) Another possibility is to take the unfalsified parameter set closest to the current control parameter set as new control parameter set. This results in less ‘aggressive’ switching, however, these parameters might become falsified more easily (because they are already on the bound of falsification).
- (3) As an alternative to the previous option, the point where the line connecting the center of the ellipsoid and the current control parameter set crosses the border of the ellipsoidal unfalsified region can be chosen (which not necessarily has to be the point that is closest to the current control parameter set).
- (4) Also an unfalsified parameter set, minimizing some criterion (e.g., related to stability) can be chosen.

3. INTERSECTION ALGORITHM

In (Pronzato and Walter, 1994) an algorithm is given to compute the minimum-volume outer-bounding ellipsoid of an intersection of the general ellipsoid $\mathcal{E}(t_{k-1})$ and a degenerate ellipsoid $\mathcal{F}(t_k)$. Five cases are distinguished:

- (1) $\mathcal{E}(t_{k-1})$ and $\mathcal{F}(t_k)$ do not intersect: an empty intersection results (Fig. 2(a)).
- (2) $\mathcal{E}(t_{k-1})$ is entirely contained in $\mathcal{F}(t_k)$: the intersection $\mathcal{E}(t_k)$ trivially is $\mathcal{E}(t_{k-1})$.
- (3) $\mathcal{E}(t_{k-1})$ is intersected by only one hyper-plane of $\mathcal{F}(t_k)$ (Fig. 2(b)).
- (4) $\mathcal{E}(t_{k-1})$ is intersected by both hyper-planes of $\mathcal{F}(t_k)$ (Fig. 2(c)).
- (5) $\mathcal{E}(t_{k-1})$ is, symmetrically around the center, intersected by both hyper-planes of $\mathcal{F}(t_k)$ (Fig. 2(d)).

3.1 Ellipsoid-with-Parallel-Cuts algorithm

Consider the ellipsoid $\mathcal{E}(t_{k-1})$, with its center defined by the vector $\theta_c(t_{k-1})$ and its shape by the matrix $\Sigma(t_{k-1})$:

$$\mathcal{E}(t_{k-1}) = \{\theta \mid (\theta - \theta_c(t_{k-1}))^T \Sigma^{-1}(t_{k-1}) \cdot (\theta - \theta_c(t_{k-1})) \leq 1\} \quad (8)$$

Introduce variables y_k and ϕ_k

$$y_k = \frac{L(s)y(t_k)}{\Delta(t_k)} \quad (9)$$

$$\phi_k = \frac{L(s)G_m(s)w(u(t), y(t))}{\Delta(t_k)} \quad (10)$$

such that, according to (5):

$$\mathcal{F}(t) = \{\theta \mid -1 \leq y_k - \phi_k^T \theta \leq 1\} \quad (11)$$

For the Ellipsoid-with-Parallel-Cuts algorithm, define

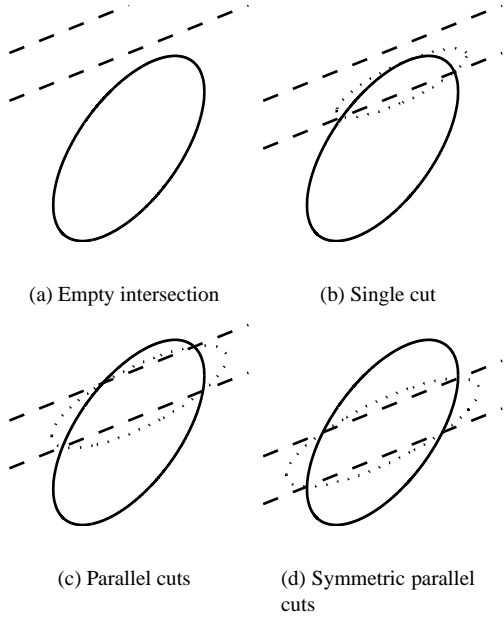


Fig. 2. Examples (2 dimensional) of possible intersections of $\mathcal{E}(t_{k-1})$ (solid line) and $\mathcal{F}(t_k)$ (dashed line). Resulting intersection $\mathcal{E}(t_k)$ is shown with a dotted line.

$$a_+ = \frac{\nu - 1}{\sqrt{g}} \quad (12)$$

$$a_- = \frac{-\nu - 1}{\sqrt{g}} \quad (13)$$

with

$$\nu = y_k - \phi_k^T \theta_c(t_{k-1}) \quad (14)$$

$$g = \phi_k^T \Sigma(t_{k-1}) \phi_k \quad (15)$$

The indicators a_+ and a_- correspond to the algebraic distance of $\theta_c(t_{k-1})$ to the bounds defined by the unfalsification criterion, in the metric defined by $\Sigma(t_{k-1})$. If $a_+ > 1$ or $a_- > 1$ the intersection is empty and the algorithm should be terminated. If $a_+ < -1$ and/or $a_- < -1$, the corresponding bound does not cut the ellipsoid and the computed intersection will not be optimal. To obtain the optimal intersection, replace a_+ and/or a_- by -1 . Furthermore, if $a_+ a_- \geq 1/p$ with p the number of parameters, the ellipsoid $\mathcal{E}(t_{k-1})$ is the optimal one and should be maintained.

If $a_+ \neq a_-$, compute the ellipsoid by

$$\Sigma(t_k) = \delta \left(\Sigma(t_{k-1}) - \frac{\sigma}{g} \Sigma(t_{k-1}) \phi_k \phi_k^T \Sigma(t_{k-1}) \right) \quad (16)$$

$$\theta_c(t_k) = \theta_c(t_{k-1}) + \frac{\sigma(a_+ - a_-)}{2\sqrt{g}} \Sigma(t_{k-1}) \phi_k \quad (17)$$

with

$$\delta = \frac{p^2}{p^2 - 1} \left(1 - \frac{a_+^2 + a_-^2 - \rho/p}{2} \right) \quad (18)$$

$$\sigma = \frac{1}{p+1} \cdot$$

$$\left[p + \frac{2}{(a_+ - a_-)^2} \left(1 - a_+ a_- - \frac{\rho}{2} \right) \right] \quad (19)$$

$$\rho = \sqrt{4(1 - a_+^2)(1 - a_-^2) + p^2(a_+^2 - a_-^2)^2} \quad (20)$$

If $a_+ = a_- = a$, σ in (19) becomes unbounded. Use the *centrally symmetric parallel cut algorithm* instead:

$$\Sigma(t_k) = \frac{p(1 - a^2)}{p - 1} \left(\Sigma(t_{k-1}) - \frac{1 - pa^2}{(1 - a^2)g} \Sigma(t_{k-1}) \phi_k \phi_k^T \Sigma(t_{k-1}) \right) \quad (21)$$

$$\theta_c(t_k) = \theta_c(t_{k-1}) \quad (22)$$

It should be noted that the volume of the ellipsoidal intersection, as calculated in this section, will never increase, as can be seen from the fact that $\Sigma(t_{k-1}) \geq \Sigma(t_k) \geq 0$. Furthermore, the ellipsoid $\mathcal{E}(t_k)$ includes only points that are either in $\mathcal{E}(t_{k-1})$ or in $\mathcal{F}(t_k)$ (and includes all points that are both in $\mathcal{E}(t_{k-1})$ and in $\mathcal{F}(t_k)$). Also, the volume is minimal, so convergence is fast.

4. SIMULATION

A simulation is performed, using the same settings as in (Cabral and Safonov, 2003): reference model $G_m(s) = \frac{1}{s+1}$, reference $r(t) = \text{sign}(\cos(0.1\pi t))$, vector field $w(u(t), y(t)) = [u(t), \frac{1}{s+1}u(t), y(t), \frac{1}{s+1}y(t)]^T$ and unstable “true but unknown plant”

$$\begin{cases} \dot{x} = \begin{bmatrix} 0 & -1 \\ 1 & 1 \end{bmatrix} x + \begin{bmatrix} 1 \\ 0 \end{bmatrix} u + \begin{bmatrix} n_1 \\ n_2 \end{bmatrix} \\ y = [0 \ 1] x \end{cases} \quad (23)$$

where n_1 and n_2 are uncorrelated normally distributed random signals with zero mean and variance one. The plant has initial state $x = 0$.

The simulation is initiated with the controller $\theta^*(0) = \theta_c(0) = [1, 0, 0.1, -0.1]^T$ and $\Sigma(0) = \text{diag}([1, 10, 10, 10])$, with a sample frequency of 1.0 kHz. Threshold $\Delta = e^{-0.05t} + 0.1$ and filter $L(s) = \frac{1}{s+1}$.

Each sample time, the ellipsoidal unfalsified region is computed, and it is checked whether $\theta^*(t_{k-1})$ is unfalsified. If not, $\theta^*(t_k)$ is updated according to scenario 3 in section 2.4:

$$\theta^*(t_k) = \theta_c(t_k) + \frac{\theta^*(t_{k-1}) - \theta_c(t_k)}{\sqrt{(\theta^*(t_{k-1}) - \theta_c(t_k))^T \Sigma^{-1}(t_k) (\theta^*(t_{k-1}) - \theta_c(t_k))}} \quad (24)$$

In Fig. 3 the results of the simulation are shown. As can be seen in Fig. 3(a), tracking performance within

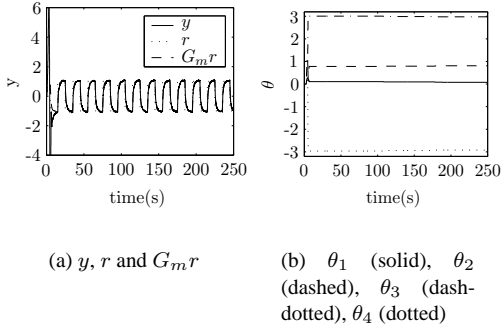


Fig. 3. *Simulation results.*

the permitted error bound is achieved. The parameter values as a function of time are shown in Fig. 3(b). It should be noted that, although a similar response is observed as in (Cabral and Safonov, 2003), the parameters converge to different values. This might be caused by differences in performance specification or in the algorithms, or because the current control parameter set is just one set from the unfalsified region (however, the final parameter set from (Cabral and Safonov, 2003) is not in the unfalsified region in this simulation).

5. EXPERIMENT

The algorithm, as presented in section 2 and 3, is implemented using a regular dSpace DS1102 controller board with a sample frequency of 1.0 kHz. The average turnaround time is 0.57 ms. The experimental setup is a dual rotary 4th order motion system, as shown in Fig. 4. It consists of a load which is connected to a motor by a thin, flexible bar. The angular position of the load is measured by an encoder and is denoted y_2 . The input to the motor is denoted u . The frequency response function (FRF) of input u to output y_2 is shown in Fig. 5.

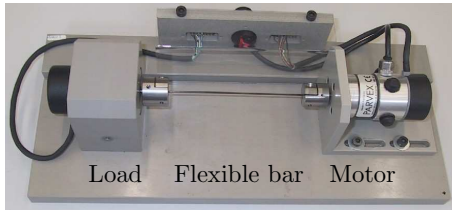


Fig. 4. *Photo of the dual rotary 4th order motion system.*

Settings for the experiment are:

$$G_m(s) = \frac{100\pi^2}{s^2 + 16\pi s + 100\pi^2} \quad (25)$$

$$w(u(t), y_2(t)) = \begin{bmatrix} u(t) \\ \frac{1}{s + 10\pi} u(t) \\ y_2(t) \\ \frac{1}{s + 10\pi} y_2(t) \end{bmatrix} \quad (26)$$

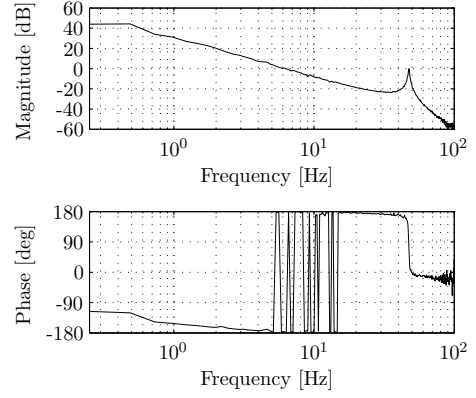


Fig. 5. *FRF of the input u to the angular position of the load y_2 .*

$$r(t) = 10 \sin(2\pi t) \quad (27)$$

$$\Delta(t) = 0.05 + 2e^{(-0.1t)} \quad (28)$$

$$\Sigma(0) = 10^3 \mathbb{I}_4 \quad (29)$$

$$L(s) = 1 \quad (30)$$

The experiment is initiated with $\theta^*(0) = \theta_c(0) = [1, 1, 1, -50]$. As in the simulation, the control parameter set is updated using (24) once it is falsified. Coulomb and viscous friction compensation is applied during the experiment.

In Fig. 6, the tracking error $G_m r - y_2$ is shown, together with the thresholds $+\Delta(t)$ and $-\Delta(t)$. As can be seen from (5) and (1), the current control parameter set is unfalsified if the tracking error is within these two thresholds (for $L(s) = 1$). If the current control parameter set is falsified, a new unfalsified control parameter set is selected. This can be seen in Fig. 7, in which the control parameter values are shown as a function of time. In Fig. 8 it is shown that the volume of the unfalsified region steadily decreases.

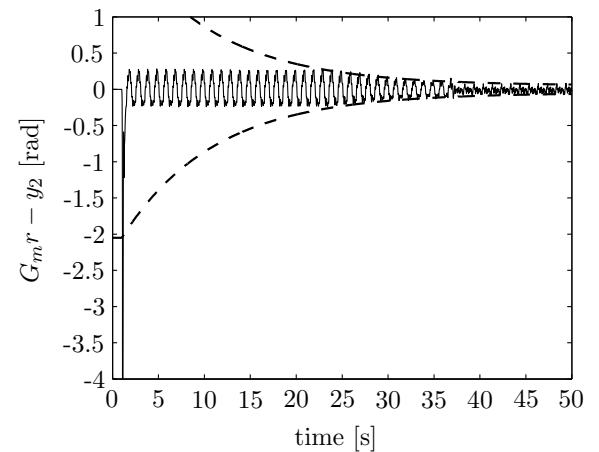


Fig. 6. *Tracking error $G_m r - y_2$ during the experiment, together with the thresholds $+\Delta(t)$ and $-\Delta(t)$. As long as $G_m r - y_2$ is within the bounds, the current control parameter set is unfalsified.*

In Fig. 9 a Bode plot is shown of the open loop of the system, with the unfalsified controller obtained after 50 seconds. As can be seen, a bandwidth of around

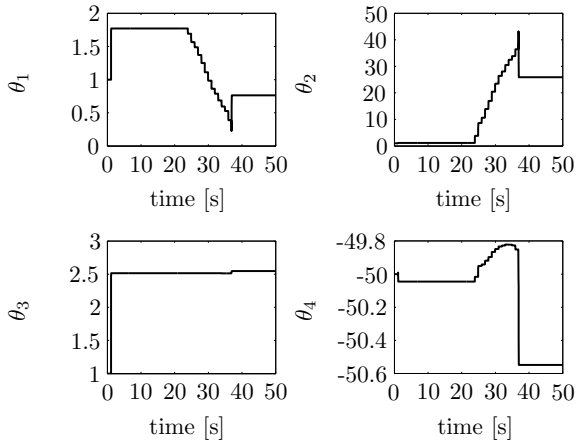


Fig. 7. Values of control parameters during the experiment as a function of time. The values change if the current control parameter set is falsified.

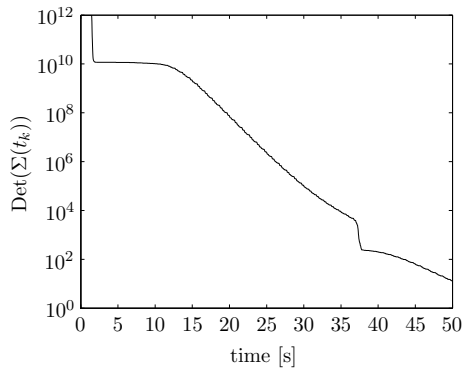


Fig. 8. Determinant of $\Sigma(t_k)$, which is proportional to the volume of $\mathcal{E}(t_k)$, as a function of time. As can be seen, $\Sigma(t_{k-1}) \geq \Sigma(t_k) \geq 0$.

10 Hz is achieved, with a phase margin of 40° (at 10 Hz) and a gain margin of 9 dB (at 42 Hz). However, it can also be seen that the resonance at 48 Hz peaks through the 0 dB line, causing only 15° phase margin at 46 Hz. The controlled system is stable but the sensitivity is bad at the resonance peak. However, due to the sinusoidal reference signal of 1 Hz, this frequency-range is not excited and hence it will not result in a large tracking error. Results with a more exciting reference signal (e.g., a block signal) are still subject of research, as well as incorporation of an unfalsified friction compensator.

6. CONCLUSION

In this paper, an unfalsified control strategy is proposed, which uses an ellipsoidal unfalsified region. The performance specification is defined as an ℓ_∞ specification, which is an ellipsoid that degenerates into two half-spaces. It is shown that by using an ellipsoidal unfalsified region and this performance specification, the update of the unfalsified region can be computed analytically. The algorithm was implemented on a dSpace DS1102 controller board at a sample frequency of 1.0 kHz (average turnaround time of 0.57

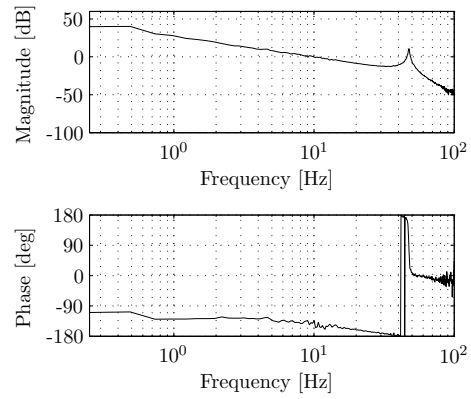


Fig. 9. Bode plot of the open loop transfer with the unfalsified controller obtained after 50 s.

ms) to control a dual rotary 4th order motion system. Experimental results are presented.

The proposed update algorithm ensures that the volume of the unfalsified region will never increase and that the ellipsoid $\mathcal{E}(t_k)$ includes only points that are either in $\mathcal{E}(t_{k-1})$ or in $\mathcal{F}(t_k)$. Minimal volume, so fast convergence, is realized.

REFERENCES

- Boyd, S., L. El Ghaoui, E. Feron and V. Balakrishnan (1994). *Linear Matrix Inequalities in System and Control Theory*. Vol. 15. SIAM studies in Applied Mathematics. Philadelphia.
- Cabral, F.B. and M.G. Safonov (2003). Unfalsified model reference adaptive control using the ellipsoid algorithm. In: *Proc. 42nd Conf. Decision & Control*. Maui, Hawaii, USA. pp. 3250–3255.
- Henrion, D., S. Tarbouriech and D. Arzelier (1998). LMI approximations for the radius of the intersection of ellipsoids. In: *Proc. 37th Conf. Decision & Control*. Tampa, Florida, USA. pp. 1759–1764.
- Katsaggelos, A.K., J. Biemond, R.W. Schafer and R.M. Mersereau (2001). A regularized iterative image restoration algorithm. *IEEE Trans. Signal Process.* **39**(4), 914–929.
- Maksarov, D.G. and J.P. Norton (1996). State bounding with ellipsoidal set description of the uncertainty. *Internat. J. Control* **65**(5), 847–866.
- Pronzato, L. and E. Walter (1994). Minimal volume ellipsoids. *Internat. J. Adapt. Control Signal Process.* **8**, 15–30.
- Ros, L., A. Sabater and F. Thomas (2002). An ellipsoidal calculus based on propagation and fusion. *IEEE Trans. Systems Man Cybernet.* **32**(4), 430–442.
- Safonov, M.G. and T.-C. Tsao (1994). The unfalsified control concept and learning. In: *Proc. 33rd Conf. Decision & Control*. Lake Buena Vista, Florida, USA. pp. 2819–2824.
- Safonov, M.G. and T.-C. Tsao (1997). The unfalsified control concept and learning. *IEEE Trans. Automatic Control* **42**(6), 843–847.